JOURNAL OF CATALYSIS **175,** 80–92 (1998)
ARTICLE NO. CA981980

The Preparation of High-Surface-Area Zirconia

II. Influence of Precipitating Agent and Digestion on the Morphology and Microstructure of Hydrous Zirconia

G. K. Chuah,[1] S. Jaenicke, and B. K. Pong

Department of Chemistry, National University of Singapore, Kent Ridge, Singapore 119260

Received August 20, 1997; revised November 24, 1997; accepted November 24, 1997

High-surface-area zirconia can be prepared by precipitation from zirconium salts. The initial product from precipitation is a hydrous zirconia of composition $ZrO(OH)_2$. The properties of the final product, zirconia, are affected by digestion of the hydrous zirconia. Hence, the aim of this study is to investigate the effects of digestion on this hydrous zirconia. It was found that hydrous oxides digested at 100°C were thermally more stable than undigested ones or samples aged in the mother liquor at room temperature. Therefore, the high surface area of the digested hydrous oxides could be retained in the resulting zirconia. The digested samples had larger pores and higher porosity than the undigested hydrous oxide. Digestion at high pH results in thicker walls in the mesoporous material, which enhances thermal stability. The higher solubility of the hydrous zirconia at pH 14 as compared to pH 9 results in faster Ostwald ripening, by which the initially amorphous samples were transformed into a crystalline material. Upon digestion at pH 14, the hydrous oxide became more dehydrated with only 0.3 to 0.5 moles of water per ZrO_2. Samples digested at pH 9 did not lose structural water. The water loss leads to a material with considerable (long range) order. The increased order manifests itself in the absence of a "glow exotherm" that is otherwise observed when the energy-rich amorphous hydrous oxide transforms on heating into a crystalline material.

INTRODUCTION

Zirconium oxide (zirconia) is attracting interest in catalysis as a support material as well as a catalyst (1). For a number of reactions, the use of zirconia as a support has been reported to give good activity and selectivity. Similar to alumina, zirconia has amphoteric properties. In many cases, better selectivity or activity has been reported when comparisons are made. For example, copper supported on zirconia gives a higher yield of methanol from CO_2 and H_2 than oxides such as alumina, silica, titania, chromium oxide, and zinc oxide (2). Chromium oxide supported on zirconia has very high activity for CO oxidation by molecular oxygen and nitrous oxide. In contrast, chromium oxide supported on silica or alumina supports was significantly less active (1). Zirconia-supported nickel prepared by coprecipitation is a good catalyst for Fischer–Tropsch synthesis. Compared with traditional supports, it exhibits a greater selectivity for higher hydrocarbons, especially olefins (3). Zirconia-supported metal oxides show higher activity for methanol oxidation than alumina- and silica-supported oxides (4). Sulfated zirconia is a solid superacid that can promote the isomerization of hydrocarbons (5–8).

Among the desired properties of a support, high surface area and thermal stability rank very high. Common supports like silica and alumina can be prepared with surface areas of 100–600 m^2/g. In contrast, commercially available zirconia has typically less than 50 m^2/g. Moreover, silica and alumina maintain their high surface area up to temperatures around 1000°C while the surface area of zirconia generally drops when the material is heated above 500°C. Like alumina or silica, zirconia shows polymorphism. Below 1100°C, the thermodynamically stable form is the monoclinic modification. However, at room temperature, zirconia is usually found in the metastable tetragonal form or as a mixture of the monoclinic and the tetragonal modifications. The transformation of the metastable tetragonal modification into the monoclinic form is generally complete by 650 to 700°C. Zirconia is a rather "new" support material and the effect of the crystal structure on catalytic activity has not yet been fully studied. Comelli *et al.* (9) attempted to investigate the influence of the crystal structures of sulfated zirconia on butane isomerization. However, despite starting with different crystalline zirconia, only the tetragonal phase could be obtained after sulfating and calcination. Hence, such studies are frequently hampered by the fact that the presence of foreign ions generally favors the formation of the metastable tetragonal structure. Transformation to the monoclinic phase occurs over a range of temperatures,

[1] To whom correspondence should be addressed. Fax: (65) 779 1691. E-mail: chmcgk@nus.sg.

0021-9517/98 $25.00

often in the regime of catalytic interest. The availability of phase-pure, stable high surface area zirconia will be very helpful for studies correlating crystal structure and catalytic activity.

Zirconium hydroxide or "hydrous zirconia" is the key intermediate in the preparation of zirconia. It can be formed using various salts such as zirconium chloride and nitrate or from alkoxides. By changing the pH during formation (10, 11), rate of addition of base (12), use of hydrothermal conditions (13, 14), presence of surfactants (15–17), and addition of other cations or anions (18–21), zirconia with different physical and structural properties is obtained. While there are many reports on the properties of zirconia, only limited studies have been carried out on the hydrous oxide. This is because the hydrous oxide usually exists in an amorphous state. Clearfield (22) was the first to report crystalline hydrous zirconia formed by refluxing zirconyl chloride solution or a slurry of freshly precipitated zirconia. He obtained X-ray diffraction patterns that indicate that the crystalline hydrous oxides were structurally almost identical to the calcined zirconia. The basic unit of the hydrous oxide is believed to be the tetrameric polycation, $[Zr(OH)_2 \cdot 4H_2O]_4^{8+}$. Hydrous zirconia forms by polymerization of these tetrameric species via olation (OH group linked to two metal atoms) to form two-dimensional sheets. These evolve into three-dimensional particles via oxolation. The rate of addition of the base, pH, and temperature are believed to affect the degree of order within the sheets.

Mamott *et al.* (23) used a dynamic diffraction technique to show that the pH of the liquid in contact with the hydrous oxide precipitate affects the temperature and rate at which the amorphous precursor transforms to crystalline zirconia. A temperature of 450°C was observed for 50% crystallization when the zirconium hydroxide was prepared at pH 9.8, while this temperature was 610°C for material prepared at pH 8.1. The transformation of the initially formed metastable tetragonal to the monoclinic phase was also found to depend on the pH of preparation, with a higher pH effecting an earlier and more complete transformation. The authors proposed that a higher pH promotes a faster polymerization of the tetrameric units. The resulting material is amorphous but contains numerous small units of two- or three-dimensional ordered assemblages. These act as nuclei for crystallization of the oxide. Using neutron thermodiffractometry, the high scattering/diffraction background due to incoherent scattering by hydrogen was used to monitor the chemical composition of the hydroxide during calcination to form zirconia (24). A cooperative process was observed in hydroxides precipitated at high pH, where simultaneous oxolation of the residual OH bridges occurs at ~500°C, resulting in rapid crystallite growth.

We have previously reported that digestion of hydrous zirconia in the mother liquor improved several properties of the calcined product, zirconia (25, 26). These include increased surface area, improved thermal stability, preferential formation of the metastable tetragonal phase, and a shift to higher temperature for the tetragonal to monoclinic phase transformation. Zirconia was formed by precipitation of zirconium chloride at pH between 9–14. The surface area and crystal phase of the zirconia were found to depend on the base used. With NH_4OH, a longer digestion time brought about an increase in the amount of the tetragonal phase. In KOH, a mixture of tetragonal and monoclinic phases (~80% : 20%) was obtained, while with NaOH, the zirconia obtained was purely tetragonal. The surface area of zirconia prepared in NH_4OH increased with digestion time and showed no maximum up to 192 h. If zirconia was prepared by digestion of the hydrous oxide at pH 14, a maximum in the surface area was found for digestion times of 12–24 h.

In order to understand how the properties of the final zirconia depend on the preparation method, it is necessary to investigate the effects of the preparation method on the hydrous oxide. Hence, we have focused our attention on the hydrous oxide. The structures of the hydrous oxide formed with NH_4OH, KOH, and NaOH as precipitating agents are compared. To determine if the crystal phase of the resulting zirconia is already decided at the time of precipitation or if it can be changed by the post-precipitation treatment, experiments were made to separate the effect of the precipitating agent from the subsequent treatment of the hydrous oxide.

METHODS

Batch 1—Influence of Precipitating Agent and Digestion Time

The preparation of hydrous zirconia by the hydrolysis of zirconium chloride with excess base has been described previously (25). A 10% solution of zirconium chloride was slowly added with a peristaltic pump to the well-stirred precipitating solution (NH_4OH, KOH, or NaOH; 5 M, *ca.* 50% excess base) at room temperature. After the addition of all the zirconium chloride, the base concentration is 0.55 M. One portion of the precipitate (0 h) was immediately removed. The rest was placed in a round-bottomed Pyrex flask and refluxed at 100°C in the supernatant liquid. Samples were removed after 12, 24, 48, 96, and 192 h. For KOH and NaOH, and pH during digestion was close to 14 (calculated pH 13.7) whereas with NH_4OH as precipitating agent, the pH was initially 11, but decreased to 9.4 at the end of the reaction. The influence of the cation—sodium, potassium, and ammonium—on the hydrous zirconia can be assessed from this batch.

Batch 2—Influence of Postprecipitation Treatment

Hydrous zirconia was formed by precipitation of zirconium chloride with excess 5 M NH_4OH. It was divided into

four portions. One portion was kept in the mother liquor (pH 9.4) while the remainder was washed with dilute ammonium nitrate solution. When no more chloride was detected in the washings (silver nitrate test), the precipitate was rinsed with deionized water. The absence of chloride in the precipitate was confirmed by X-ray fluorescence (Link XR200). The precipitate was then divided into three portions (~10 g each) and redispersed in 250 ml of 5 M NH_4OH (pH 11), KOH, and NaOH (pH 14.7), respectively. One sample from each portion was left to age at room temperature for 192 h while the rest was subjected to digestion at 100°C for various lengths of time. This experiment will give an insight into whether the observed crystallographic properties of the resulting zirconia are primarily determined by the precipitation step or whether they can be altered by subsequent treatment. In the former case, the same crystal structure should be observed in the hydrous oxide, irrespective of the digestion/aging medium. The effect of chloride can be studied by comparing with the hydrous oxides digested in the chloride-containing mother liquor (Batch 1 or 2-NH_3/Cl-series).

After digestion, the solids of Batch 1 were recovered and washed free of chloride. For Batch 2 samples that were already free of chloride, the same amount of ammonium nitrate solution was used as for the chloride-containing samples. The samples were then dried overnight at 100°C. The thermal stability of the hydrous oxides was assessed in terms of a change in surface area after heating in a muffle furnace to temperatures between 100 and 500°C for 1 h. To transform the precursors to zirconia, the hydrous oxides were calcined at 500°C for 12 h. A heating rate of 1°C/min was used in all cases to reach the final temperature. Samples were cooled to 100°C at 20°C/min.

The following codes are used to identify the hydrous zirconia from the two batches. For Batch 1, the code is 1-*X*-*y*-P with $X = NH_3$, K, or Na for precipitation/digestion medium of NH_4OH, KOH, or NaOH, respectively; *y* the digestion time in hours; and P for precursor. For Batch 2, the code is 2-*X*-AP, where $X = NH_3$/Cl, NH_3, K, or Na and refers to the post-precipitation treatment in the mother liquor, or 5 M of pure NH_4OH, KOH, or NaOH, respectively; and AP identifies the precursor aged for 192 h at room temperature. Hydrous oxides that were digested at 100°C are referred to as 2-*X*-*y*-P with *y* the digestion time in hours.

Characterization

Thermogravimetric analysis (Dupont SDT 2960) and differential scanning calorimetry (Dupont DSC 2920) were performed on the hydrous oxides. A heating rate of 20°C/min was used for both TGA and DSC analyses with a gas flow of 80 ml/min of air and nitrogen, respectively. To ensure that the sample was thoroughly dry and free of physically bound water, each sample was held isothermally at 100°C for 30 min before ramping up to 600 or 900°C during the DSC to TGA run, respectively. The dry weight of the sample was determined at the end of the DSC measurement and used in the calculation for the specific heat evolved.

Surface areas were determined using a Micromeritics Flowsorb 2300. Nitrogen adsorption/desorption isotherms and the pore volumes were measured with a Quantachrome NOVA 2000. Very careful degassing of the samples is necessary so that all water is removed from the pores but physical changes to the sample are avoided. The incomplete removal of physisorbed water will result in a low surface area or an erroneous pore size measurement. Degassing of the hydrous zirconia for about 50 min at 100°C in a flow of nitrogen or nitrogen/helium mixture is found to be sufficient for the removal of physically adsorbed water. X-ray diffractograms were measured using a Siemens D5005 diffractometer (Cu anode) equipped with variable primary and secondary beam slits. Crystallite sizes were estimated using the Debye–Scherrer equation,

$$D_{hkl} = \frac{0.9\lambda}{\beta_{hkl} \cdot \cos\theta}, \qquad [1]$$

where D_{hkl} is the crystallite size, λ is the wavelength of the CuK_α radiation, β_{hkl} is the peak width corrected for instrumental broadening, and θ is the Bragg diffraction angle.

RESULTS

Elemental Analysis

During digestion, the hydrous oxides are in contact with excess precipitating agent. Adsorbed/absorbed cations and anions may affect the microstructural and morphological properties of the material. In Batch 1, the anions were hydroxide and chloride while the cation—potassium, sodium, or ammonium—differed for the different precipitants used. Elemental analysis showed that sodium and some potassium ions were present in the hydrous oxides only after digestion at around pH 14 (Table 1). Freshly precipitated materials could be washed free of the monovalent cations. The hydrous oxides digested in NaOH (1-Na-series) contained 0.75 to 1.36 wt% sodium with negligible amounts of potassium. Sodium was also present in the KOH-digested samples (1-K-series). The probable source of sodium is as an impurity (0.5 wt%) with the KOH. For Batch 2, no chloride was present in the digestion medium of the 2-NH_3-, 2-K-, and 2-Na-series. However, the concentration of hydroxide ions was higher than in the 2-NH_3/Cl-series or Batch 1 as the mother liquor had been substituted with 5 M of the pure base. The digested samples of the 2-K-series contained 0.48–0.76 wt% sodium, which is higher than the ~0.25 wt% detected in the 1-K-series. The 2-Na-digested hydrous oxides contained 0.67–1.1 wt% sodium, similar to that of the 1-Na-series. The aged hydrous oxides, 2-K-AP and 2-Na-AP, contained 0.17 and 0.24 wt% sodium, respectively.

TABLE 1

Sodium and Potassium Concentration in Hydrous Zirconia from Batches 1 and 2

Sample	Na (wt%)	K (wt%)	Sample	Na (wt%)	K (wt%)
1-K-0-P	0.002	0.002	1-Na-0-P	0.018	0.000
1-K-12-P	0.24	0.064	1-Na-12-P	0.75	0.020
1-K-24-P	0.26	0.070	1-Na-24-P	0.80	0.020
1-K-48-P	0.25	0.094	1-Na-48-P	0.88	0.026
1-K-96-P	0.26	0.16	1-Na-96-P	0.97	0.001
1-K-192-P	0.25	0.55	1-Na-192-P	1.36	0.001
2-K-AP	0.17	0.021	2-Na-AP	0.24	0.002
2-K-12-P	0.48	0.025	2-Na-12-P	0.67	0.001
2-K-24-P	0.55	0.081	2-Na-24-P	0.74	0.007
2-K-48-P	0.65	0.080	2-Na-48-P	0.86	0.025
2-K-96-P	0.75	0.082	2-Na-96-P	0.98	0.020
2-K-192-P	0.77	0.078	2-Na-192-P	1.11	0.040

Crystallinity of Hydrous Zirconia

Irrespective of the precipitating agent, the undigested hydrous zirconia was X-ray amorphous. Only after digestion in KOH or NaOH did crystallinity develop in the hydrous oxides (26). In Batch 1, the hydrous zirconia digested in KOH was a mixture of the tetragonal and monoclinic phase, with 75–85% tetragonal (Table 2). The crystallites of both phases were very small, 30–60 Å. Hydrous oxides that were digested in NaOH were purely tetragonal, with crystallites around 40–50 Å. Despite calcination to 500°C, no change in the crystal phase or crystallite size was observed in the digested samples from the 1-K- and 1-Na-series. In contrast, the digested hydrous oxides from the 1-NH_3-series remained X-ray amorphous even after digestion for 192 h. However, the effects of digestion on these hydrous oxides became apparent in the crystalline material that is obtained after calcination at 500°C. Zirconia from the undigested precursor was predominantly monoclinic, 84%. The monoclinic crystallites were ~127 Å while the tetragonal crystallites were much smaller, ~43 Å. With increasing digestion time, the proportion of tetragonal phase increased; however, the crystallite size decreased (Fig. 1). The size of the tetragonal crystallites in 1-NH_3-12-500 was ~100 Å, but in 1-NH_3-96-500, it was only 63 Å. 1-NH_3-192-500 remained X-ray amorphous even after a calcination time of 12 h.

TABLE 2

Crystalline Phase of the Hydrous Oxide Precursors from Batches 1 and 2

Sample	Tetragonal (%)	Sample	Tetragonal (%)
1-K-0-P	Amorphous	1-Na-0-P	Amorphous
1-K-12-P	75.2	1-Na-12-P	100
1-K-24-P	82.5	1-Na-24-P	100
1-K-48-P	84.9	1-Na-48-P	100
1-K-96-P	75.3	1-Na-96-P	100
1-K-192-P	80.8	1-Na-192-P	100
2-K-AP	Amorphous	2-Na-AP	Amorphous
2-K-12-P	100	2-Na-12-P	100
2-K-24-P	100	2-Na-24-P	100
2-K-48-P	100	2-Na-48-P	100
2-K-96-P	100	2-Na-96-P	100
2-K-192-P	100	2-Na-192-P	100

Note. 1-NH_3-, 2-NH_3/Cl-, and 2-NH_3-hydrous oxides were all amorphous.

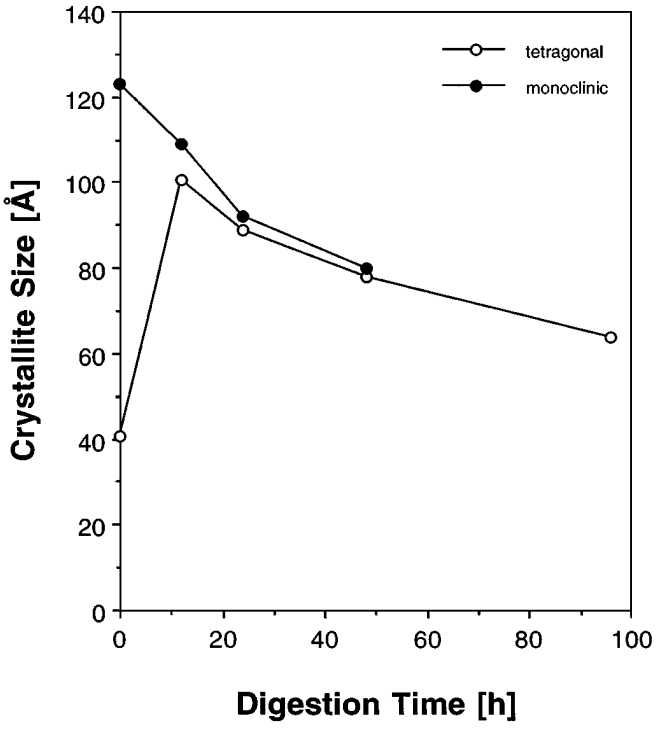

FIG. 1. Crystallite sizes of the monoclinic and tetragonal phase in zirconia calcined at 500°C from the 1-NH_3-series.

Despite the long aging time of 192 h, the aged hydrous oxides from Batch 2 remained X-ray amorphous with the exception of 2-Na-AP. The X-ray diffraction pattern of 2-Na-AP showed a very broad peak centered at 2θ ~30°, indicating a certain degree of crystallinity (Fig. 2). After calcination of the hydrous oxides, both 2-NH_3/Cl-AP and 2-NH_3-AP transformed to mostly monoclinic zirconia. The tetragonal phase constitutes only 14.3 and 15.8%, respectively. The distribution of the crystalline phases was similar in zirconia prepared from the freshly precipitated precursor, where the tetragonal phase amounted to 16.2%. Thus, aging at pH 9–11 did not cause much change in the structure of the hydroxide. In contrast, aging at room temperature in strong base, KOH and NaOH, led to a remarkable increase in the proportion of tetragonal crystals in the calcined zirconia, to 87.5 and 90.0%, respectively. Although the initial precipitate was the same in all cases, the presence of strong alkalis had significantly altered the hydrous oxide so that the resulting zirconia crystallizes preferentially in the tetragonal phase.

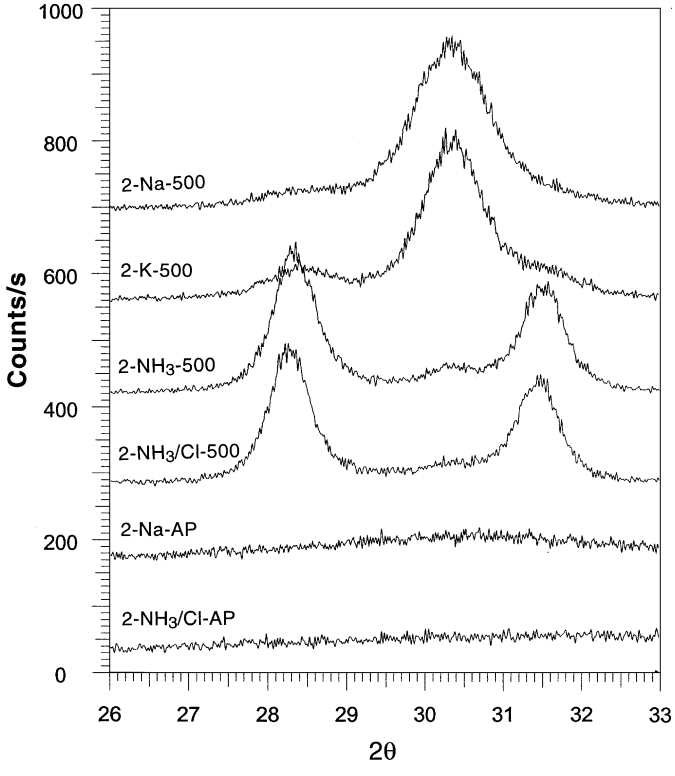

FIG. 2. XRD of aged hydrous oxides and the resulting zirconia calcined at 500°C. The curves have been offset for clarity.

Digestion of the hydrous oxides in the chloride-free bases at 100°C gave rather similar results to that of Batch 1. Both the 2-K- and 2-Na-hydrous oxides became crystalline showing only the tetragonal phase. In contrast, the 1-K-samples contained a small proportion of monoclinic crystallites. The 2-NH_3/Cl- and 2-NH_3-hydrous oxides remained X-ray amorphous even after digestion. A comparison with the aged hydrous oxides shows that heating at 100°C speeds the reaction so that crystallization is observed in a shorter time. After calcination to 500°C, the crystal phase of the zirconia from 2-Na- and 2-K-series remained purely tetragonal. Similar to Batch 1, zirconia from the 2-NH_3/Cl- and 2-NH_3-series showed an increasing proportion of the tetragonal phase with digestion time; the latter had a higher fraction of the tetragonal form. Hence, the results show that the crystal structure formed after precipitation can be altered by exposure to different pH.

Thermogravimetric Analysis

Thermogravimetric analysis (TGA) and DSC measurements were performed on the hydrous zirconia. The observed weight loss is entirely due to the removal of water (27). 1-K-0-P, 1-Na-0-P, and 1-NH_3-0-P lost approximately 1 mole water per ZrO_2 (Table 3). Therefore, the undigested hydrous oxides have the formula $ZrO_2 \cdot H_2O$ or $ZrO(OH)_2$. However, hydrous oxides of the 1-K- and 1-Na-series which had been digested at 100°C lost less water during TGA. The water content in these samples was between 0.33 and 0.55 H_2O per ZrO_2, irrespective of the length of digestion. In contrast, precursors from the 1-NH_3-series lost about 1 mole water per ZrO_2 during TGA to 500°C whether they had been digested or not.

The DSC curves show a continuous broad endotherm from room temperature to about 300°C. This is due to the water loss from the hydrous precursor (12). Between 400 and 500°C, a large exothermic peak known as the glow exotherm (28, 29) is frequently observed in the DSC of hydrous zirconia. For Batch 1, both 1-K-0-P and 1-Na-0-P exhibit this phenomenon. The enthalpy, ΔH, was 17.4 and 17.0 kJ/mole ZrO_2 for 1-K-0-P and 1-Na-0-P, respectively. Digested samples of the 1-K- and 1-Na-series did not show any glow exotherm even when heated to 600°C. For the 1-NH_3-series, the glow exotherm was observed in 1-NH_3-0-P, 1-NH_3-12-P, 1-NH_3-24-P, and 1-NH_3-48-P (Fig. 3). However, the peak maximum moved to increasingly higher temperatures while the enthalpy decreased from 19.7 kJ/mole in 1-NH_3-0-P to 12.7 kJ/mole in 1-NH_3-48-P. Samples digested for more than 48 h did not show any exotherm up to 600°C (the instrumental limit of the equipment).

From the weight loss, the stoichiometry of the aged hydrous oxides, 2-NH_3/Cl-AP and 2-NH_3-AP, was determined

TABLE 3

TGA and DSC of Hydrous Zirconia

Sample	Amount of water lost [mole/mole ZrO_2 formed]	Glow exotherm ΔH [kJ/mole ZrO_2]	Glow exotherm Temperature [°C]	E_a[a] [kJ/mole]	$E_a + \Delta H$ [kJ/mole]
1-K-0-P	1.07	17.4	435	176	193
1-K-12-P	0.33	—	—	—	—
1-K-24-P	0.35	—	—	—	—
1-K-48-P	0.38	—	—	—	—
1-K-96-P	0.44	—	—	—	—
1-K-192-P	0.40	—	—	—	—
1-Na-0-P	0.89	17.0	420	172	189
1-Na-12-P	0.40	—	—	—	—
1-Na-24-P	0.39	—	—	—	—
1-Na-48-P	0.42	—	—	—	—
1-Na-96-P	0.55	—	—	—	—
1-Na-192-P	0.45	—	—	—	—
1-NH_3-0-P	0.90	19.7	450	180	200
1-NH_3-12-P	0.92	18.0	489	189	207
1-NH_3-24-P	0.85	17.2	517	197	214
1-NH_3-48-P	0.82	12.7	563	209	222
1-NH_3-96-P	0.89	—	—	—	—
1-NH_3-192-P	0.79	—	—	—	—
2-NH_3/Cl-AP	1.16	22.5	450	180	200
2-NH_3-AP	1.13	17.4	450	180	197
2-K-AP	0.86	11.3	411	170	181
2-Na-AP	0.84	4.31	412	170	174

[a] Calculated from Redhead equation.

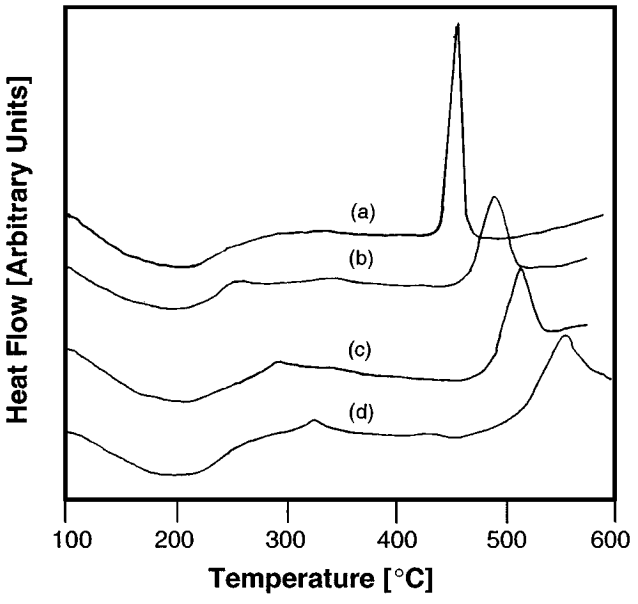

FIG. 3. DSC scans of hydrous oxides (a) 1-NH_3-0-P, (b) 1-NH_3-12-P, (c) 1-NH_3-24-P, and (d) 1-NH_3-48-P.

as $ZrO_2 \cdot H_2O$, similar to that of the freshly precipitated material. However, after aging in 5 M KOH or NaOH, the water content of the hydrous oxide was reduced to ~0.85 mole per ZrO_2. Therefore, at pH 14.7, the condensation of hydroxyl groups with elimination of water appears to occur to a higher degree. A glow exotherm was observed for all the aged precursors (Fig. 4); however, the heat evolved was highest for 2-NH_3/Cl-AP and 2-NH_3-AP with 22.5 and 17.4 kJ/mole, respectively. The precursor aged in KOH had an exotherm of 11.3 kJ/mole while 2-Na-AP showed an exotherm of only 4.30 kJ/mole. The maximum of the exotherm moved from 450°C in the NH_3-aged samples to 411°C for hydrous oxides aged at pH 14.

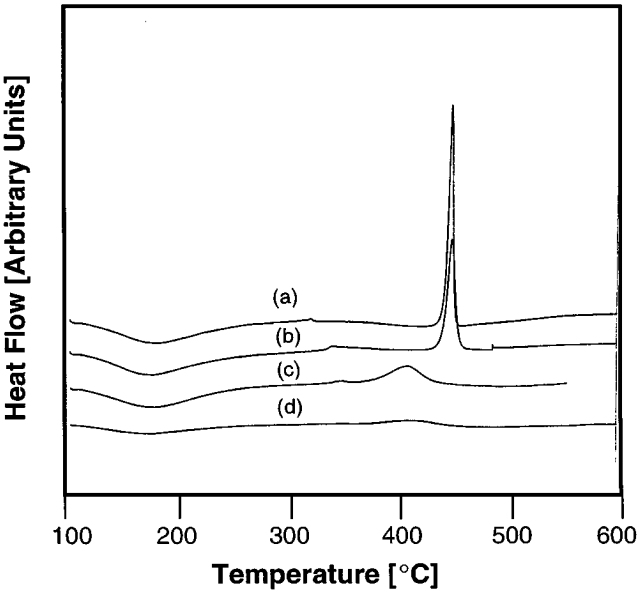

FIG. 4. DSC scans of hydrous oxides (a) 2-NH_3/Cl-AP, (b) 2-NH_3-AP, (c) 2-K-AP, and (d) 2-Na-AP.

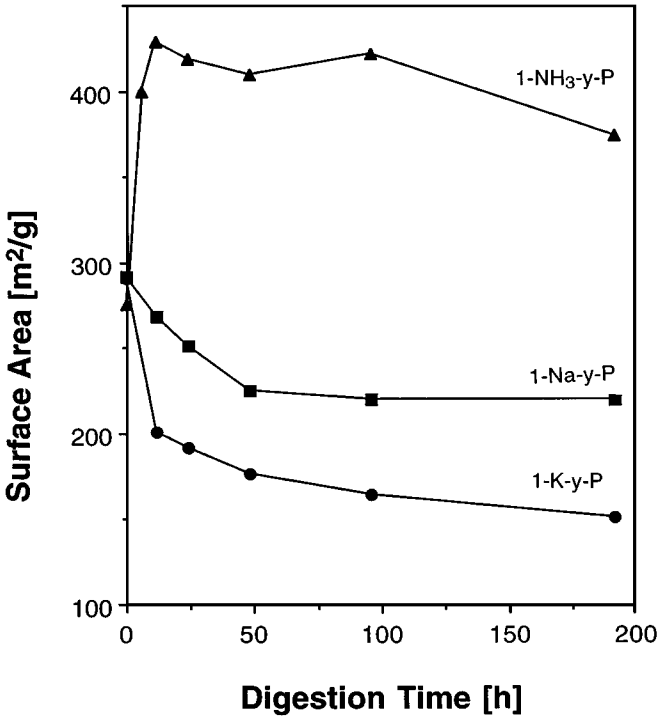

FIG. 5. Surface area of the hydrous oxides from Batch 1 versus time of digestion.

Thermal Stability of the Hydrous Oxide

The undigested hydrous oxide, 1-K-0-P, had a surface area of 291 m^2/g. The surface area decreased with digestion time, so that 1-K-192-P had only 151 m^2/g (Fig. 5). Figure 6 shows the surface area of the hydrous oxides from the 1-K-series as a function of drying temperature up to 500°C. Digested hydrous oxides did not suffer any significant loss in surface area. The surface area of these samples remained unchanged even after the heating time at 500°C was extended from 1 to 12 h. The undigested hydrous oxide, however, lost surface area rapidly with temperature, especially above 300°C. After 1 h at 500°C, the surface area was only 65.4 m^2/g and decreased further to 39.8 m^2/g when calcined for 12 h. Both 1-K-12-P and 1-K-24-P formed zirconia with the highest surface area, 195 m^2/g, after calcination at 500°C for 12 h.

The 1-Na-hydrous oxides (Fig. 7) showed a similar behavior to that of the 1-K-series, although the surface areas of all digested hydrous oxides were higher (220–268 m^2/g). The surface area of the digested samples remained stable up to 500°C but the undigested sample, 1-Na-0-P, lost its surface area rapidly. The maximum surface area in the resulting zirconia (250 m^2/g) was obtained from hydrous oxides that had been digested between 12 and 24 h. The surface

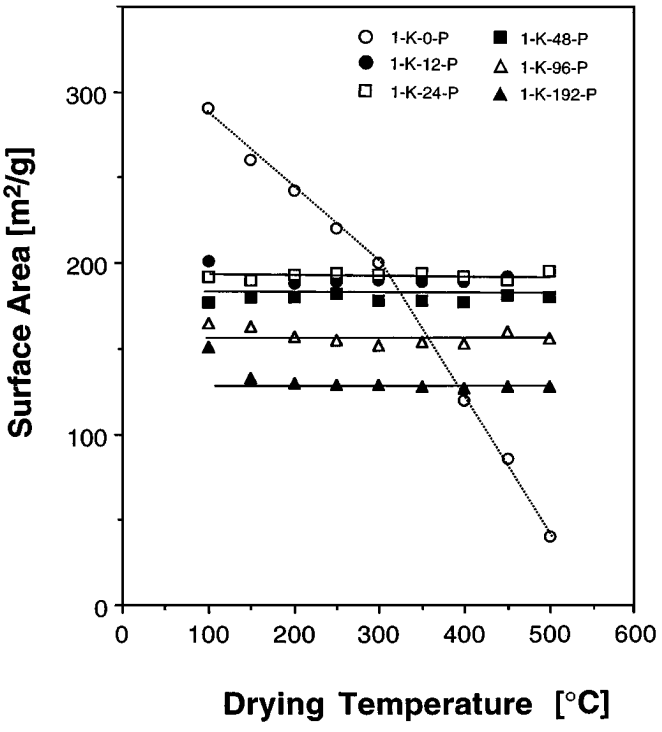

FIG. 6. KOH-digested samples: surface area of the hydrous oxides versus drying temperature.

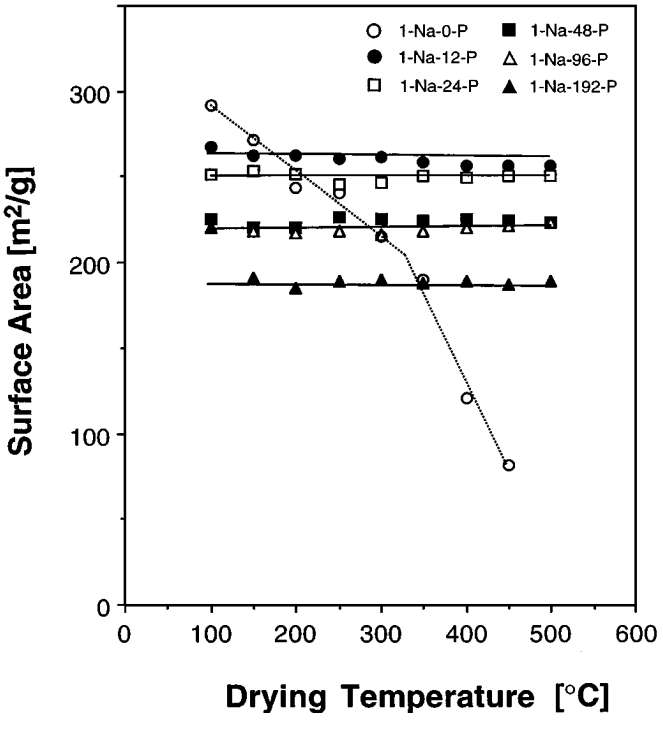

FIG. 7. NaOH-digested samples: surface area of the hydrous oxides versus drying temperature.

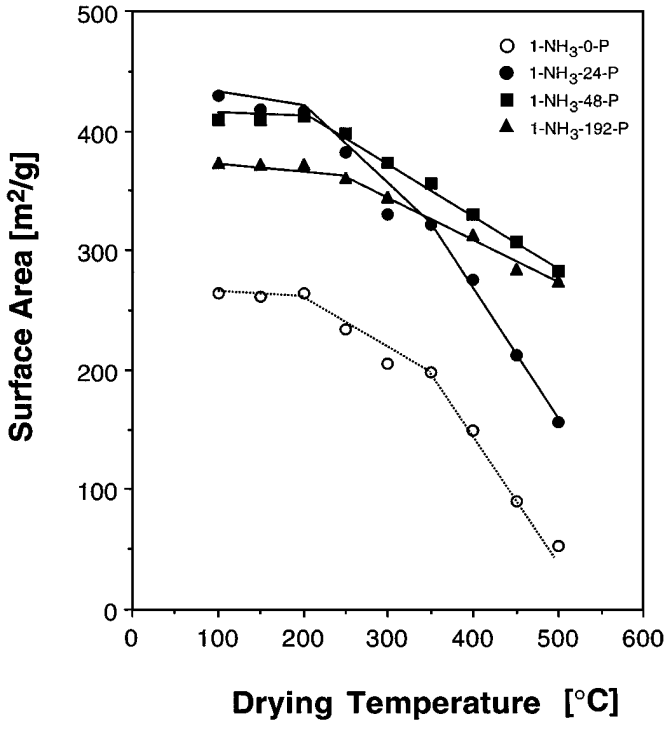

FIG. 8. NH_4OH-digested samples: surface area of the hydrous oxides versus drying temperature.

area decreased for longer digested samples and was only 160 m^2/g for 1-Na-192-500.

The NH_3-precipitated sample, 1-NH_3-0-P, had a surface area of 264 m^2/g after drying at 100°C. Digestion at pH 9 resulted in an increase in the surface area of the hydrous oxides to 370–430 m^2/g. However, when these samples were heated, they lost their high surface area whereas the corresponding samples from the 1-K- or 1-Na-series were much more stable (Fig. 8). The degree of surface area loss depends on the length of time to which the samples had been digested: longer-digested samples were thermally more stable than those digested for shorter times. Consequently, the surface area of the resulting zirconia in the NH_3-series increased with the digestion time of the hydrous oxide. 1-NH_3-0-500 had a surface area of only 42.8 m^2/g but 1-NH_3-192-500 had a very high surface area of 240 m^2/g. With the three precipitants, different digestion times are required in order to obtain zirconia with maximum surface area. A shorter digestion time of 12 to 24 h is sufficient when KOH or NaOH is used, but a much longer time is needed with NH_4OH.

Aged hydrous oxides had surface areas similar to those of the freshly precipitated material, in the range 240–280 m^2/g (Table 4). After calcination at 500°C for 12 h, the zirconia formed had low surface areas, similar to those formed from the freshly precipitated precursor. We conclude that aging of the hydrous oxide at room temperature does not help to achieve a higher surface area in the resulting zirconia.

TABLE 4

Surface Area of Aged Hydrous Oxides and the Resulting Zirconia

Sample	Surface area [m^2/g]
Hydrous zirconia, aged	
2-NH_3/Cl-AP	242
2-NH_3-AP	283
2-K-AP	258
2-Na-AP	270
Zirconia, calcined at 500°C	
2-NH_3/Cl-500	40.2
2-NH_3-500	44.6
2-K-500	52.2
2-Na-500	55.9

The surface area of the digested hydrous oxides from Batch 2 showed a dependence on digestion time similar to that shown by the Batch 1 samples. The zirconia formed from the digested hydrous oxides were better stabilized against loss of surface area during calcination and hence had up to 250 m^2/g depending on the alkali of the digestion medium and the digestion time.

Pore Structure

Nitrogen adsorption/desorption isotherms were measured for the hydrous zirconia. The isotherms of the undigested samples are similar in shape, regardless of the precipitant, to the hysteresis loop resembling that of type H2 of the IUPAC nomenclature (Fig. 9). Such isotherms are characteristic for systems with open or closed pores of variable radius (30). They have also been associated with ink-bottle pores where the entrance to the pores is narrower than the body. As a consequence of digestion, the shape of the adsorption/desorption isotherms gradually changed from type H2, which was observed for samples digested up to 12 h, to one resembling a H1-type. The type H1 loop is typical for agglomerates or compacts of spherical particles with fairly uniform size or for open-ended cylindrical pores.

The pore size distribution is calculated by the Barrett–Joyner–Halenda (BJH) method (30). For digested samples, the desorption branch of the isotherm was used for the calculations whereas the adsorption branch was used for undigested samples. For type H2 isotherms, the desorption of nitrogen is limited by the narrow neck of the pore and information about the body of the pore can only be obtained from an analysis of the adsorption isotherm. In all undigested samples, including those aged at room temperature from Batch 2, the average pore diameter was ~25 Å. No maximum was noted in the curves (Fig. 10).

Mesopores developed only after digestion. In 1-K-12-P, the pores had an average diameter of ~56 Å (Table 5). The size increased with longer digestion so that 1-K-192-P had pores in the range 60 to 500 Å with the average around 240 Å. The distribution curve also broadens with digestion time. A similar effect was also observed for digested hydrous oxides of the NaOH-series. For the 1-NH_3-series, all the digested samples had very similar pore diameters (Fig. 11). A slight increase from 80 Å in 1-NH_3-24-P to 100 Å in 1-NH_3-192-P was observed.

The total pore volume, V_p, has been determined from the amount of nitrogen adsorbed at a relative pressure close to unity, based on the assumption that the pores are then filled with liquid adsorbate (Gurvitsch Rule). The results are shown in Table 5. The pore volume of the undigested precursors is around 0.18–0.19 ml/g. This value is similar to that found by Mercera *et al.* (31) for their hydrous oxide which had been aged in the mother liquor at pH 10 for 65 h. Digestion brought about a significant increase in the pore volume. For the 1-K- and 1-Na-series, the pore volume increased by more than threefold after 192 h digestion. In the NH_3-series, the pore volume increased to 0.81 ml/g in 1-NH_3-192-P.

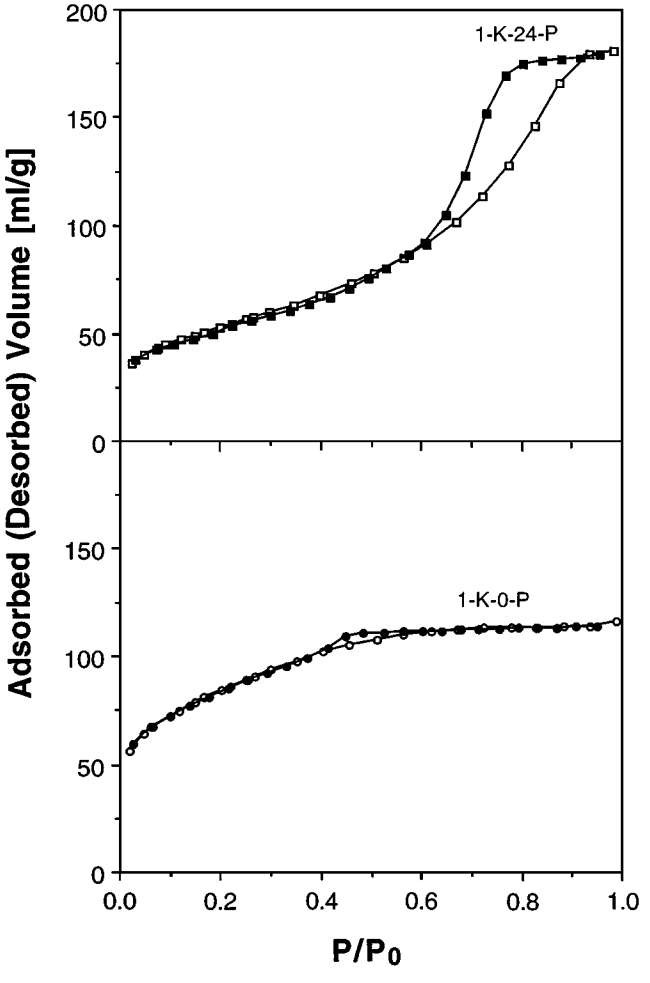

FIG. 9. N_2 adsorption/desorption isotherms at 77 K for 1-K-0-P and 1-K-24-P.

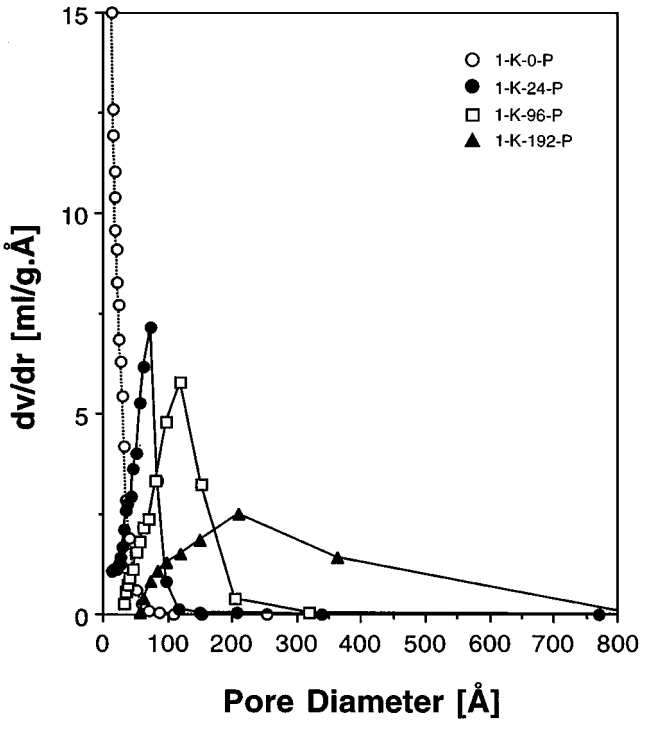

FIG. 10. Pore size distribution for hydrous oxides digested in KOH.

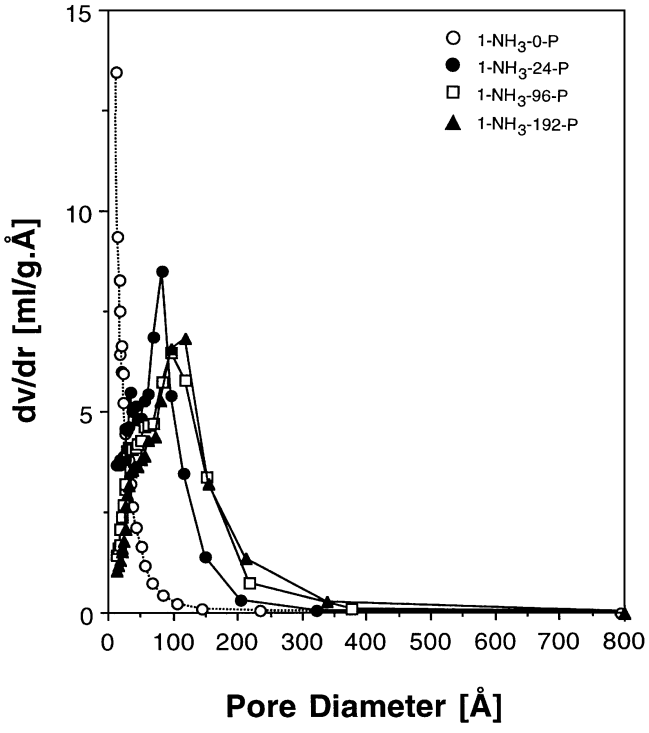

FIG. 11. Pore size distribution curves for hydrous oxides digested in NH_4OH.

Based on the pore volume and the mean pore radius, an estimate was made of the wall thickness in the hydrous zirconia (Table 5). For a model of a long cylinder (length l) with uniform pore size (radius r) and a wall thickness dr, the following equations apply,

$$l = V_p/\pi r^2 \quad [2]$$

$$V_{solid} = l \cdot \pi \cdot [(r + dr)^2 - r^2] = 1/\rho, \quad [3]$$

where the density of zirconia is taken as 6.0 g/ml.

Equating l from the two equations, we have

$$dr = \sqrt{r^2 + \frac{\pi r^2}{6V_p}} - r. \quad [4]$$

As the hydrous zirconia exists as particles rather than as a single long cylinder, the wall thickness between the pores is $2dr$. For 1-K-0-P, a wall thickness of 24 Å is obtained, but this increased with digestion to 78 Å in 1-K-192-P. A similar trend is observed for the NaOH-series where the wall thickness increased from 24 Å in 1-Na-0-P to 54 Å in 1-Na-192-P. However, for the 1-NH_3-series, no significant change in wall thickness was observed for the digested samples (28–30 Å) as compared to 1-NH_3-0-P (29 Å). For the digested samples that were crystalline, the crystallite size determined using X-ray diffraction agrees well with the calculated wall thickness (Table 5).

TABLE 5

Pore Volume, Mean Pore Diameter, and Calculated Wall Thickness for Hydrous Zirconia

Sample	Pore volume [ml/g]	Mean pore ϕ [Å]	Estimated wall thickness $2dr$ [Å]
1-K-0-P	0.1800	24.6	24.1
1-K-12-P	0.2279	56.4	46.0
1-K-24-P	0.2822	67.0	46.2
1-K-48-P	0.4238	93.3	46.2
1-K-96-P	0.4858	121	53.4
1-K-192-P	0.6714	235	78.5
1-Na-0-P	0.1886	25.2	23.8
1-Na-12-P	0.3111	51.6	32.9
1-Na-24-P	0.4391	65.3	31.4
1-Na-48-P	0.5086	95.4	40.5
1-Na-96-P	0.5282	120	49.3
1-Na-192-P	0.6319	153	53.9
1-NH_3-0-P	0.1906	30.4	28.5
1-NH_3-24-P	0.6379	81.0	28.3
1-NH_3-48-P	0.6403	81.0	28.2
1-NH_3-96-P	0.7689	99.9	29.6
1-NH_3-192-P	0.8116	104	29.4

DISCUSSION

Based on the above results, the following model for the role of digestion on the hydrous zirconia is proposed. Freshly precipitated or aged (at room temperature)

hydrous zirconia consists of a loose agglomeration of primary particles with a diameter of ~20 Å. In alkaline solution, these particles are negatively charged and repel each other. During digestion, the higher temperature leads to increased thermal agitation. Collisions between the charged particles occur at a higher rate than at room temperature. This enhances the formation of surface bonds between particles by condensation of surface hydroxyl groups. Thermogravimetry showed that digested hydrous oxides were "drier" than the freshly precipitated hydrous oxide. The loss of water from the hydrous zirconia indicates that increasing condensation between hydroxyl groups has taken place. It has been proposed by Clearfield (32, 33) that polymerization of the hydrous zirconia leads to three-dimensional structures with the formula $[ZrO_x(OH)_{4-2x} \cdot yH_2O]_n$. Thereby, a network of particles with higher porosity than in the undigested sample forms. For both the 1-NH_3- and 1-Na-series, a rapid increase in the porosity is observed for digestion up to 24 h while for the 1-K-series, the pore volume increased up to 48 h; thereafter, a smaller increase was observed.

In addition to the network formation by coalescence of primary particles, another effect of the higher temperature is the dissolution and reprecipitation of material which helps in strengthening the network of particles. The local solubility is smaller at the neck joining two particles than at the surface of the particle (34). Preferential deposition of zirconia at the necks leads to thickening in these areas. It is then possible to remove the water from the pores without collapse of the network structure. Undigested samples do not form a stabilized network because of electrostatic repulsion between the charged particles. The pore size distribution for the undigested samples does not show a maximum but decreases monotonously from very small to larger pores. Hence, it can be envisaged that during drying, the coagulated particles collapse and form a dense structure. The pore space then corresponds to the void space between the (spherical) particles in an almost close packing. The precipitates are X-ray amorphous indicating that the size of the primary particles, R, is smaller than 20–30 Å. The pores in a random packing of such spheres will have radii starting from ~3 Å.

Our results indicate that the dissolution/redeposition is enhanced at pH ~14 as compared to pH 9. This is in agreement with the thermodynamic calculations of Denkewicz *et al.* (14), who showed that the solubility of zirconium hydroxide at pH 9 is smaller than at pH 14 by a factor of 10^4. The wall thickness of samples that had been digested at pH ~14 increased with digestion time. Before digestion, the wall thickness of the hydrous oxides was estimated as only 20–30 Å, but after digestion for 192 h, it increased to about 50–70 Å. This increase in wall thickness and average pore size together with a relatively small increase in pore volume indicates that walls separating the smaller pores disappear during digestion and this material is redeposited on the walls of the bigger pores. Therefore, a decrease in the internal surface is expected because of digestion. This is indeed the case for the 1-K- and 1-Na-series, where after an initial period of 24 h, the surface areas of the hydrous oxides decreased with longer digestion time. Hydrous oxides digested at the lower pH of 9 do not show thickening of the walls despite digestion for a long time. Also, the mean pore size remains essentially unchanged with digestion time. Obviously, dissolution and deposition of material occur at a slower rate at this pH. The thinner walls in the 1-NH_3-series are the cause for the reduced thermal stability of these samples compared to the 1-K- and 1-Na-series. However, even within the 1-NH_3-series, the trend is that the longer-digested samples are better able to withstand higher temperatures. We assume that this is the result of greater crystalline perfection in these samples. The most frequently occurring type of defects in zirconia is Schottky defects consisting of pairs of cation and anion vacancies (21). A more defect-free structure is expected as digestion progresses. Diffusional mass transport will be reduced in the longer-digested samples so that nucleation and grain growth are hindered.

Information about the local atomic ordering in the hydrous oxide can be deduced from differential scanning calorimetry. The transformation of the hydrous oxide to zirconia is usually accompanied by a highly exothermic peak, the glow exotherm. Various explanations have been put forth to explain the origin of this exotherm including the transformation of an amorphous material to the tetragonal phase or to the monoclinic structure. Srinivasan *et al.* (12) found that irrespective of the final crystal phase obtained, the exotherm occurred at the same temperature and with the same enthalpy. We observe the glow exotherms only in those samples that were initially X-ray amorphous but transformed to a crystalline state upon calcination, e.g., the undigested samples. It is absent when a crystalline hydrous oxide (e.g., hydrous oxides digested at pH 14) transforms to a crystalline oxide or an amorphous hydrous oxide (e.g., long-digested NH_3-samples) forms an amorphous zirconia. Hence, the presence of the exotherm is clearly related to a change from short-range ordering to long-range ordering of the atoms. The measured enthalpy corresponds to the energy difference between the hydrous oxide and zirconia. Since the final state is essentially at the same energy, a higher enthalpy implies a more disordered precursor state. The freshly precipitated hydrous oxide is in a state of high energy due to its random structure. By digestion, localized order sets in, lowering the energy. Thus, the exotherm decreased with digestion time for a precursor digested at pH 9 where the material was still X-ray amorphous. We use the term "glassy" to describe this annealed state. At high pH, and especially under conditions of digestion, nucleation and crystal growth lead to long-range order as shown by

crystalline peaks in the XRD spectra. Hence, these precursors have an even lower energy than those digested at pH 9 and transform to zirconia with no measurable exotherm.

The activation energy for crystallization, E_a, can be estimated from the peak temperature of the glow exotherm by using the Redhead equation (35),

$$E_a = RT_p[\ln(vT_p/\beta) - 3.64], \quad [5]$$

where v is taken as 10^{13} s^{-1}, T_p is the peak temperature, β is the heating rate, and R is the gas constant. Table 3 shows that the activation energy of crystallization for the undigested hydrous oxide is 172–180 kJ/mole. The activation energy of hydrous oxide digested in NH_4OH increases to 189–209 kJ/mole with digestion time. However, the sum of the activation energy and enthalpy is not a constant but increased from ~200 kJ/mole in the freshly precipitated sample to 220 kJ/mole for hydrous oxide digested up to 48 h. This shows that as the hydrous oxide becomes more stable with digestion, the energy of the activated complex on the path toward crystallization to zirconia also increases. These results indicate the increasing difficulty in forming nucleation sites in the "glassy" state (Fig. 12a). As a more defect-free structure is formed by digestion, the atomic

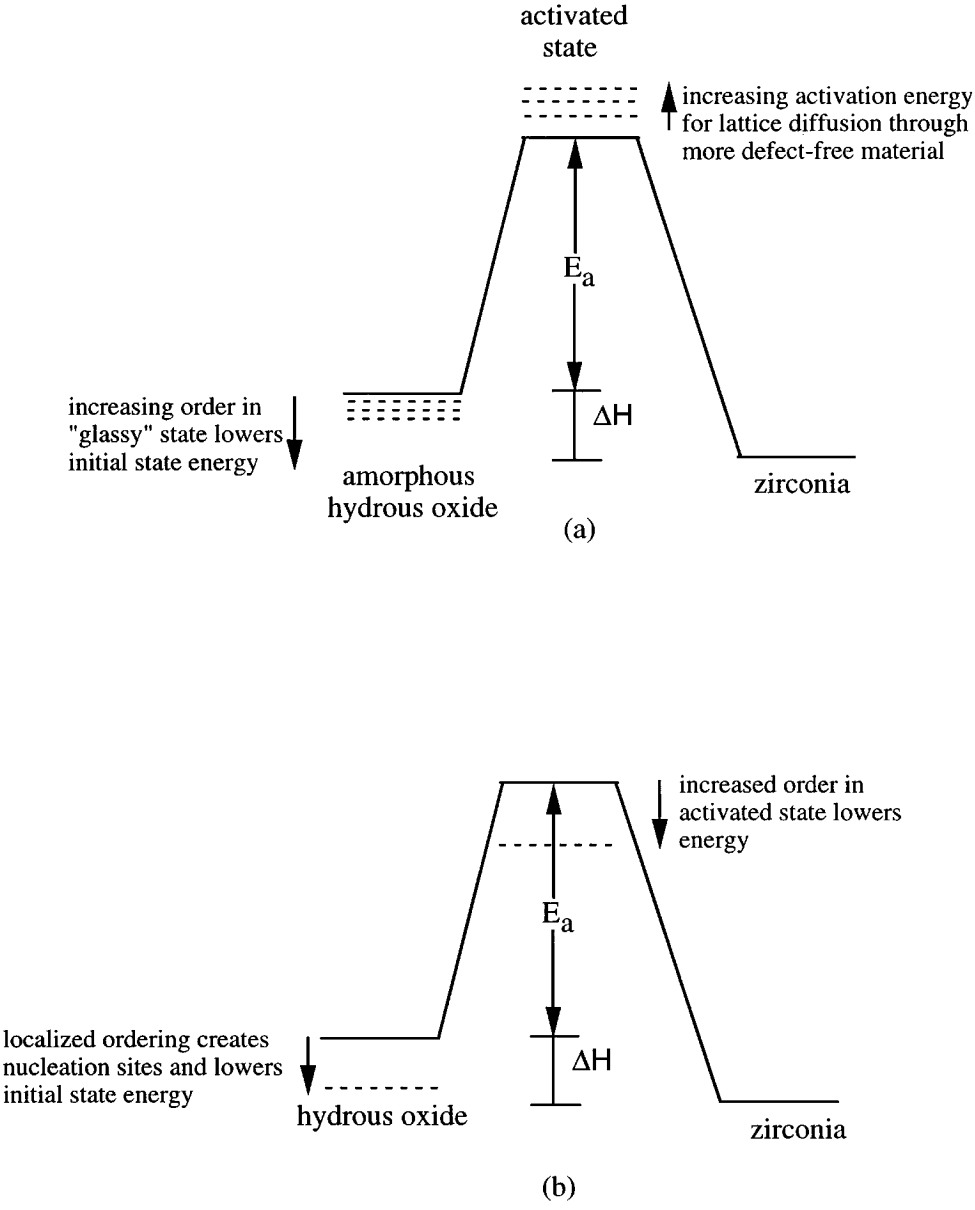

FIG. 12. Schematic energy diagrams (a) digestion at pH 9: the glow enthalphy (ΔH) is reduced but the activation energy for crystallization (E_a) increases with digestion; (b) aging (digestion) at pH 14: both the glow exotherm and activation energy are reduced due to extensive ordering and nucleation.

diffusion necessary for nucleation and crystallization becomes more difficult. In the extreme case of samples 1-NH_3-96-P and 1-NH_3-192-P, no glow exotherm was observed at all, and these samples were X-ray amorphous even after calcination at 500°C. The enthalpy of transformation and the activation energy of crystallization are both reduced for hydrous oxides kept at pH 14, even at room temperature (Batch 2). This may be attributed to the more extensive localized ordering within the polymeric structure in this pH regime so that more nucleation sites are formed (23). These hydrous oxides have an energy only slightly above that of the crystalline zirconia, which results in a very weak glow exotherm. The activation energy toward crystallization is also low and reflects more the process of crystal growth than nucleation (Fig. 12b).

The formation of the metastable tetragonal phase in zirconia has been explained by a number of effects such as lower surface excess energy of the tetragonal than of the monoclinic phase (35), the adsorption of oxygen at surface anionic sites initiating the monoclinic to tetragonal transformation (36), etc. The presence of foreign ions such as sodium is known to cause preferential formation of the tetragonal phase. We have reported that uptake of sodium in the hydrous oxide occurs preferentially over potassium even when the latter is in excess (26). Digested hydrous oxides from 2-K-series were purely tetragonal while those from 1-K-series consisted of some 20% monoclinic phase. This may be related to the higher hydroxide concentration in the digestion medium of the 2-K-series. It is impossible to decide whether the hydroxide concentration affects the crystal phase formation directly or indirectly via increased adsorption of sodium. It is known that at pH >7, hydrous zirconia acts as a cation exchanger and the uptake of cations increases with pH. Indeed, a higher sodium content is measured for the 2-K-hydrous oxides than for the corresponding Batch 1 samples. Our results also show that the uptake increases with temperature so that digested hydrous oxides have a higher cation content than undigested ones. Chloride ions do not play any significant role at the alkaline pH of the digestion medium as shown by the similar structural data for the samples digested in chloride-free and chloride-containing NaOH or NH_4OH.

CONCLUSION

(a) Freshly precipitated hydrous oxides using NH_4OH, KOH, or NaOH are similar in the chemical formula, $ZrO_2 \cdot H_2O$. Digestion at pH 14 resulted in loss of water so that the hydrous oxides have only 0.30–0.5 mole water per ZrO_2. Digestion at pH 9 did not cause any significant dehydration of the hydrous oxides.

(b) The crystal structure of the resulting zirconia depends on the precipitating agent but can be altered by post-precipitation treatment (aging or digestion) of the hydrous oxide. The pH of the digestion medium and/or uptake of sodium plays a role in the formation of the tetragonal phase.

(c) Samples digested at pH ~14 show only a very small loss in surface area when heated to 500°C. Hence the high surface area of the hydrous oxides can be retained in the resulting zirconia. In the conversion from hydrous oxide to zirconia, samples that were digested at pH 9 for longer periods had a smaller loss in surface area than those digested for shorter times.

(d) The influence of digestion is interpreted in terms of the enhanced agglomeration of primary particles during digestion and the strengthening of the network structure which is then better able to withstand thermal treatment. Hydrous oxides digested at pH 9 are less thermally stable than those digested at pH 14.

(e) The decreased enthalpy of the glow exotherm together with the lack of X-ray crystallinity indicate the formation of a glassy state in hydrous oxides digested at pH 9. Long range ordering occurred in hydrous oxides digested at pH 14 and hence, they do not show any glow exotherm.

ACKNOWLEDGMENT

The authors gratefully acknowledge the financial support for this work (RP 950608) from the National University of Singapore.

REFERENCES

1. Yamaguchi, T., *Catal. Today* **20**, 199 (1994).
2. Amenomiya, T., *Appl. Catal.* **30**, 57 (1987).
3. Bruce, L., and Mathews, J. F., *Appl. Catal.* **4**, 353 (1982).
4. Deo, G., and Deo, G., *in* "Catalytic Selective Oxidation" (S. T. Oyama and J. W. Hightower, Eds.), p. 31, ACS Symposium Series, Vol. 523, ACS, Washington, DC, 1993.
5. Iglesia, E., Soled, S. L., and Kramer, G. M., *J. Catal.* **144**, 238 (1993).
6. Garin, F., Seyfried, L., Girard, P., Maire, G., Abdulsamad, A., and Sommer, J., *J. Catal.* **151**, 26 (1995).
7. Tichit, D., El Alami, D., and Figueras, F., *J. Catal.* **163**, 18 (1996).
8. Cheung, T.-K., Langer, F. C., and Gates, B. C., *J. Catal.* **159**, 99 (1996).
9. Comelli, R. A., Vera, C. R., and Parera, J. M., *J. Catal.* **151**, 96 (1995).
10. Davis, B. H., *J. Am. Ceram. Soc.* **67**, C168 (1984).
11. Adair, J. H., and Denkewicz, R. H., *Ceram. Powder Sci.* **3**, 25 (1990).
12. Srinavasan, R., Harris, M. B., Simpson, S. F., de Angelis, R. J., and Davis, B. H., *J. Mater. Res.* **3**, 787 (1988).
13. Adair, J. H., Denkewicz, R. P., Arriagada, F. J., and Osseo-Asare, K., *Ceram. Trans.* **1**, 135 (1988).
14. Denkewicz, R. P., Jr., TenHuisen, K. S., and Adair, J. H., *J. Mater. Res.* **5**, 2698 (1990).
15. Knowles, J. A., and Hudson, M. J., *J. Chem. Soc., Chem. Comm.*, 2083 (1995).
16. Ciesla, U., Schacht, S., Stucky, G. D., Unger, K. K., and Schüth, F., *Angew. Chem. Int. Ed. Engl.* **35**, 541 (1996).
17. Larsen, G., Lotero, E., Babity, M., Petkovic, L. M., and Shobe, D. S., *J. Catal.* **164**, 246 (1996).
18. Saha, S. K., and Pramanik, P., *British Cer. Trans.* **94**, 123 (1995).
19. Duchet, J. C., Tilliette, M. J., and Cornet, D., *Catal. Today* **10**, 507 (1991).
20. Mercera, P. D. L., Van Ommen, J. G., Doesburg, E. B. M., Burggraaf, A. J., and Ross, J. R. H., *Appl. Catal.* **71**, 363 (1991).

21. Mercera, P. D. L., Van Ommen, J. G., Doesburg, E. B. M., Burggraaf, A. J., and Ross, J. R. H., *Appl. Catal.* **78**, 79 (1991).
22. Clearfield, A., *Inorg. Chem.* **3**, 146 (1964).
23. Mamott, G. T., Barnes, P., Tarling, S. E., Jones, S. L., and Norman, C. J., *J. Mater. Sci.* **26**, 4054 (1991).
24. Turrillas, X., Barnes, P., Tarling, S. E., Jones, S. L., Norman, C. J., and Ritter, C., *J. Mater. Sci. Letts.* **12**, 223 (1993).
25. Chuah, G. K., Jaenicke, S., Cheong, S. A., and Chan, K. S., *Appl. Catal. A* **145**, 267 (1996).
26. Chuah, G. K., and Jaenicke, S., *Appl. Catal. A* **163**, 261 (1997).
27. Chan, K. S., Chuah, G. K., and Jaenicke, S., *J. Mater. Sci. Letts.* **13**, 1579 (1994).
28. Livage, J., Doi, K., and Mazieres, C., *J. Am. Ceram. Soc.* **51**, 349 (1968).
29. Gregg, S. J., and Sing, K. S. W., *in* "Adsorption, Surface Area and Porosity," 2nd ed. Academic Press, London, 1982.
30. Mercera, P. D. L., Van Ommen, J. G., Doesburg, E. B. M., Burggraaf, A. J., and Ross, J. R. H., *Appl. Catal.* **57**, 127 (1990).
31. Clearfield, A., Serrette, G. P. D., and Khazi-Syed, A. H., *Catal. Today* **20**, 295 (1994).
32. Clearfield, A., *Rev. Pure Appl. Chem.* **14**, 91 (1964).
33. Zarzycki, J., *in* "Glass Science and Technology" (D. R. Uhlmann and J. J. Kreidl, Eds.), Vol. 2, p. 209. Academic Press, New York, 1984.
34. Redhead, P. A., *Vacuum* **12**, 203 (1962).
35. Garvie, R. C., *J. Phys. Chem.* **69**, 1238 (1965).
36. Srinivasan, R., Davis, B. H., Cavin, O. B., and Hubbard, C. R., *J. Am. Ceram. Soc.* **75**, 1217 (1992).